

# CORTICO-MUSCULAR COHERENCE ENHANCEMENT VIA SPARSE SIGNAL REPRESENTATION

Yuhang Xu\*    Qi Yu†    Wei Dai†    Zoran Cvetković\*    Verity M. McClelland‡

\* Department of Informatics, King's College London, UK

† Department of Electrical and Electronic Engineering, Imperial College London, UK

‡ Department of Basic and Clinical Neuroscience, King's College London, UK

## ABSTRACT

Identification of specific cortico-muscular interactions is essential for understanding sensorimotor control. These interactions are commonly studied by analyzing cortico-muscular coherence (CMC) between electroencephalogram (EEG) and surface electromyogram (sEMG) recorded synchronously under a motor control task. However, the presence of noise and components irrelevant to the monitored task weakens CMC so that it is often very difficult to detect. This study proposes an approach based on dictionary learning and sparse signal representation combined with a component selection algorithm to extract versions of EEG and sEMG signals which contain higher relative levels of coherent components. Evaluations using neurophysiological data show that the method achieves substantial increase in CMC levels.

**Index Terms**— Cortico-muscular coherence, EEG, sEMG, sparse representation, enhancement

## 1. INTRODUCTION

Cortico-muscular coherence (CMC) analysis, which detects the presence of synchronous components in electrophysiological recordings from the brain and concurrently active muscles, is one of the most common signal processing methods used in studying the mechanisms of cortico-muscular interactions [1–3]. However, there are several factors that could make CMC so low that the synchrony between electroencephalogram (EEG) and surface electromyogram (sEMG) signals would be difficult to detect. One of the factors is the time delay between synchronized events in the brain and the muscle which can be described as the bias due to misalignment [4, 5]. The main reason for the typically low level of coherence between sEMG and EEG signals collected synchronously during controlled motor tasks is the presence of noise and activities unrelated to the task of interest [6, 7].

One approach towards increasing the level of the EEG and sEMG components relative to the considered activities is via blind source separation (BSS) techniques [8–11]. The effectiveness of these techniques increases with the increasing number of recording channels. In order to minimize

health-care costs and simplify the operation of diagnostic data collection, an approach for CMC enhancement inspired by Wavelet Independent Component Analysis (WICA) was proposed, which was particularly useful to low-channel count data [7]. In this study, we propose a denoising method based on the techniques of sparse signal representation, which could be applied to EEG and single-channel sEMG signals. The proposed method is based on the assumption that with a properly constructed dictionary and well designed sparse decomposition techniques, it is possible to represent motor-control components in EEG and sEMG signals using a few higher amplitude waveforms, while the background activity and noise will spread over many low intensity components due to the absence of structure [12]. This facilitates extracting relevant components from EEG and sEMG signals, ultimately leading to largely increased CMC levels. The effectiveness of proposed approach is illustrated by applying it to the neurophysiological signals.

The paper is organized as follows. In Section 2 the problem of sparse representation is formulated first. Then a method for further selection of components of sparse expansions is described. Experimental results are presented in Section 3. Section 4 draws some conclusions.

## 2. METHODS

### 2.1. Coherence between EEG and sEMG

During the process of movement control, the cortical signal  $x_c(t)$  corresponding to the considered activity is transmitted to the controlled muscle via multiple paths. The response  $y_c(t)$  of the muscle can thus be represented as  $y_c(t) = \sum_{j=1}^{N_x} b_j x_c(t - D_j)$ , where  $b_j$  and  $D_j$  represent the attenuation and delay, respectively, corresponding to an individual path [5]. The sEMG signal is composed of  $y_c(t)$  and noise, and has the form  $y(t) = y_c(t) + n_y(t)$ , where  $n_y(t)$  is the noise component which involves noise and various other components irrelevant to the monitored task. An analogous model for EEG can be established as the sum of muscle-control event and noise component, which has the form  $x(t) = x_c(t) + n_x(t)$ . The coherence between the

sEMG and EEG signals at a frequency  $\omega$  can be shown to have the form

$$C_{xy}(\omega) = \frac{|G_{xy}(\omega)|^2}{G_{xx}(\omega)G_{yy}(\omega)} = \frac{|B(\omega)|^2 G_{x_c x_c}^2(\omega)}{(G_{x_c x_c}(\omega) + G_{n_x n_x}(\omega))(|B(\omega)|^2 G_{x_c x_c}(\omega) + G_{n_y n_y}(\omega))}, \quad (1)$$

where  $G_{x_c x_c}(\omega)$ ,  $G_{n_x n_x}(\omega)$ ,  $G_{n_y n_y}(\omega)$  are power spectral densities of  $x_c(t)$ ,  $n_x(t)$ , and  $n_y(t)$ , and  $B(\omega)$  is the frequency response of the propagation channel. It can be observed that if the components  $n_x$  and  $n_y$  are strong compared to the components involved in cortico-muscular interaction, the coherence would be very low.

## 2.2. Sparse Representation for EEG and sEMG

Towards the enhancement of coherent components in EEG and sEMG signals, first a dictionary in which they can be represented in a sparse manner needs to be learned. The main idea of the algorithm proposed here is that structured synchronous EEG and EMG components will have sparse representation under such a common dictionary which could facilitate noise removal. Given the observed dataset  $\mathbf{R} = [\mathbf{r}_1 \ \mathbf{r}_2 \ \dots \ \mathbf{r}_m]$ ,  $\mathbf{r}_i \in \mathbb{R}^n$ , we intend to find a dictionary  $\mathbf{D} \in \mathbb{R}^{n \times k}$ , which consists of  $k$  atoms,  $\mathbf{D} = [\mathbf{d}_1 \ \mathbf{d}_2 \ \dots \ \mathbf{d}_k]$ , and a sparse enough representation  $\mathbf{S} = [\mathbf{s}_1 \ \mathbf{s}_2 \ \dots \ \mathbf{s}_m]$ ,  $\mathbf{s}_i \in \mathbb{R}^k$  subject to  $\|\mathbf{R} - \mathbf{D}\mathbf{S}\|_F^2 \leq \epsilon$  [13]. This can be achieved by finding a dictionary  $\mathbf{D}$  and a representation  $\mathbf{S}$  that solve the following optimization problem

$$\arg \min_{\mathbf{D}, \mathbf{S}} \left\{ \|\mathbf{R} - \mathbf{D}\mathbf{S}\|_F^2 + \lambda \|\mathbf{S}\|_0 \right\}, \quad (2)$$

where we use  $\|\mathbf{S}\|_0$  to denote the number of nonzero entries in  $\mathbf{S}$ . Towards finding one dictionary  $\mathbf{D}$  for simultaneously recorded EEG signal  $\mathbf{X} = [\mathbf{x}_1 \ \mathbf{x}_2 \ \dots \ \mathbf{x}_L]$ ,  $\mathbf{x}_i \in \mathbb{R}^n$  and sEMG signal  $\mathbf{Y} = [\mathbf{y}_1 \ \mathbf{y}_2 \ \dots \ \mathbf{y}_L]$ ,  $\mathbf{y}_i \in \mathbb{R}^n$ , where  $L$  is the number of trials, in which both signals have sparse representation, we form matrix  $\mathbf{R} = [\mathbf{X} \ \mathbf{Y}]$  of observations and find the dictionary by solving the problem (2) using K-SVD method, which was first presented by Aharon *et al.* [13].

The sparse representation of EEG and sEMG signals with respect to this dictionary has the form

$$\begin{aligned} \hat{\mathbf{X}} &= \mathbf{D}\mathbf{S}_x, \\ \hat{\mathbf{Y}} &= \mathbf{D}\mathbf{S}_y, \end{aligned} \quad (3)$$

where  $\mathbf{S}_x = [\mathbf{s}_{x,1} \ \mathbf{s}_{x,2} \ \dots \ \mathbf{s}_{x,L}]$ ,  $\mathbf{s}_{x,i} \in \mathbb{R}^k$  and  $\mathbf{S}_y = [\mathbf{s}_{y,1} \ \mathbf{s}_{y,2} \ \dots \ \mathbf{s}_{y,L}]$ ,  $\mathbf{s}_{y,i} \in \mathbb{R}^k$  are the sparse expansion matrices corresponding to  $\mathbf{X}$  and  $\mathbf{Y}$ , respectively. Once the dictionary  $\mathbf{D}$  is found, the sparse representation problem

above can be formulated as

$$\min_{\mathbf{s}_{x,i}, \mathbf{s}_{y,i}} \left\{ \sum_{i=1}^L \left\{ \frac{1}{2} \|\mathbf{x}_i - \mathbf{D}\mathbf{s}_{x,i}\|_2^2 + \frac{1}{2} \|\mathbf{y}_i - \mathbf{D}\mathbf{s}_{y,i}\|_2^2 + \lambda_1 \|\mathbf{s}_{x,i}\|_1 + \lambda_2 \|\mathbf{s}_{y,i}\|_1 \right\} \right\}. \quad (4)$$

The  $\ell_1$ -norm can be used to measure sparsity instead of the  $\ell_0$ -norm in order to make this optimization problem convex with respect to each of the dictionary  $\mathbf{D}$  and the sparse coding  $\mathbf{S}$  when the other one is fixed [14]. Whilst techniques of dictionary learning typically produce both sparse representations of EEG and sEMG signals as well as the underlying dictionary, in order to obtain higher accuracy of the sparse representation, we will use Alternating Direction Method of Multipliers (ADMM), which combines the benefits of both augmented Lagrangian and dual decomposition methods to solve the sparse representation problem under the obtained  $\mathbf{D}$  [15].

To that end we will reformulate the sparse representation problem (4), which is a convex optimization problem with respect to  $\mathbf{S}_x$  and  $\mathbf{S}_y$ , by introducing  $\mathbf{Z}_x = \mathbf{S}_x$ ,  $\mathbf{Z}_y = \mathbf{S}_y$ . The problem then becomes equivalent to

$$\begin{aligned} \min_{\mathbf{s}_{x,i}, \mathbf{s}_{y,i}, \mathbf{z}_{x,i}, \mathbf{z}_{y,i}} \left\{ \sum_{i=1}^L \left\{ \frac{1}{2} \|\mathbf{x}_i - \mathbf{D}\mathbf{s}_{x,i}\|_2^2 + \frac{1}{2} \|\mathbf{y}_i - \mathbf{D}\mathbf{s}_{y,i}\|_2^2 + \lambda_1 \|\mathbf{z}_{x,i}\|_1 + \lambda_2 \|\mathbf{z}_{y,i}\|_1 \right\} \right\}, \\ \text{subject to } \mathbf{z}_{x,i} = \mathbf{s}_{x,i}, \ \mathbf{z}_{y,i} = \mathbf{s}_{y,i}, \end{aligned} \quad (5)$$

where  $\mathbf{z}_{x,i}$  and  $\mathbf{z}_{y,i}$  represent the  $i$ th column vector of matrix  $\mathbf{Z}_x$  and  $\mathbf{Z}_y$ , respectively, which is then solved by ADMM [15].

It turns out that sparse representation of EEG and sEMG signals alone is not sufficient to achieve a substantial increase in CMC levels, hence we consider to perform further selection of coherent components using a greedy algorithm. The complete CMC enhancement algorithm can be summarized as follows:

- 1) **Initial sparse representation.** Perform dictionary learning on input EEG and sEMG signals to obtain the dictionary  $\mathbf{D}$  and then perform ADMM to obtain the sparse coefficient matrices  $\mathbf{S}_x$  and  $\mathbf{S}_y$ . Any entry of  $\mathbf{S}_x$  and  $\mathbf{S}_y$  below a threshold  $T$  is set to zero, and the sparse coefficient matrices become  $\mathbf{S}_x^0$  and  $\mathbf{S}_y^0$ .
- 2) **Component selection initialization.** Sparse coefficient matrix  $\mathbf{S}_x^0$  is then used as the input for coherent component selection algorithm. The initial value of CMC,  $C_{xy}^0$ , is computed as the value of CMC between EEG and sEMG signals that are reconstructed with the dictionary  $\mathbf{D}$  and the sparse coefficient matrices  $\mathbf{S}_x^0$  and  $\mathbf{S}_y^0$ . Coefficient entry counters are set to  $p = 1$  and  $q = 1$ , and the iteration counter is set to  $g = 1$ .

- 3) **Coefficient removal.** If the  $(p, q)$ th entry of sparse coefficient matrix is zero, jump to step 5), otherwise set  $\mathbf{S}_x^0(p, q) = 0$ . The sparse coefficient matrix is thus updated with the  $(p, q)$ th coefficient cleared, and EEG signal is reconstructed with the updated matrix of sparse coefficients and dictionary  $\mathbf{D}$ .
- 4) **CMC estimation and sparse coefficient decision.** The CMC between sEMG and reconstructed EEG signals is calculated. If it is higher than  $C_{xy}^{g-1}$ , the coherence  $C_{xy}^g$  to be compared next time will be updated with the value of CMC calculated between sEMG and the reconstructed EEG signals. Otherwise, if the CMC is lower than or equal to  $C_{xy}^{g-1}$ , the  $(p, q)$ th coefficient  $\mathbf{S}_x^0(p, q)$  is restored in the updated matrix of sparse coefficients and the reference coherence level is set to  $C_{xy}^g = C_{xy}^{g-1}$ .
- 5) **Iteration.** The indices are set to  $p = p + 1$  and  $q = q$  if  $p < k$  and  $q \leq L$ . Otherwise, if  $p = k$  and  $q < L$ , the indices are set to  $p = 1$  and  $q = q + 1$ . Step 3) to step 5) are repeated until all coefficients have been considered, *i.e.*  $p = k$  and  $q = L$ .
- 6) **Repeat the process with sEMG.** Reset the index to  $p = 1$  and  $q = 1$ . The whole selection process, steps 3) to 5) are repeated with  $\mathbf{S}_y^0(p, q)$ .

**Remark.** The coherence between EEG and sEMG is estimated in short-time Fourier domain in order to keep their statistical properties fairly constant over the intervals [16, 17]. Since the length of EEG and sEMG segments used for dictionary learning and sparse representation could be longer than the length of window of short-time Fourier analysis (STFA) used for coherence calculation, the highest coherence among all possible time shifts of the STFA is taken into account in the component selection decision in step 4) and in setting up the reference value in step 2) of the algorithm .

### 3. RESULTS

#### 3.1. Data Acquisition

Five healthy subjects were asked to perform a simple motor task: with their dominant hand holding a plastic ruler parallel to and above the table surface in a key grip between the thumb and index finger [18]. Pulses of lateral displacement generated by an electromechanical tapper at defined times give the subjects the sensation that their grip on the ruler may be lost. The subjects were asked to hold the ruler gently against the stylus of the tapper and maintain its position. Surface EMG was recorded using adhesive electrodes in a belly-tendon montage over first dorsal interosseous (FDI) of the dominant hand. EEG was recorded from the scalp overlying the contralateral motor cortex. EEG and sEMG were sampled at 1024 Hz, amplified and bandpass filtered (0.5 -

100 Hz for EEG; 5 - 500 Hz for sEMG). The stimuli were delivered at pseudorandom intervals varying between 5.6 s and 8.4 s (mean 7s), in order that the subject could not anticipate the arrival of the next stimulus. The stimulus of a single trial, which lasted 5 seconds, was applied 1.1 second after the start of the data collection period. A short rest was between blocks, each of which contains 25 corresponding data epochs (trials). Up to 8 blocks of data (200 trials) were collected for each subject [18].

#### 3.2. Analysis Period and Coherence Estimation

Our analysis was concentrated on the late post-stimulus period, especially around the second prominent coherence peak (Peak 2), which appears between 2.5 and 3.5 s, since there could be less bidirectional signaling and the motor control is expected to be more stable [5]. EEG and FDI segments of 128-sample, 256-sample and 512-sample length around Peak 2 were used for dictionary learning and sparse representation. Learning using segments of 256-sample length (250 ms) gave best performance, and that was chosen for this study. However, during the process of coefficient selection, the coherence between reconstructed EEG and sEMG signals was calculated using STFA windows of 128-sample length (125 ms), with time shifts of 10 samples (9.8 ms) between consecutive analysis windows, due to the desired trade-off between time and frequency resolutions [5].

#### 3.3. Coherent component enhancement

The value of coherence between EEG and sEMG that are reconstructed with their sparse expansion matrices was estimated first. We investigated the influence of  $\lambda_1$  and  $\lambda_2$  in (5) on the coherence levels, which is shown in Table 1, where  $\lambda_1 = \lambda_2 = \lambda$ . It can be observed from Table 1 that the CMC could decrease when  $\lambda$  increases, which could be due to the fact that although increasing the sparsity could remove more noise components, some useful components could be eliminated as well. Results in Table 1 also show that with  $\lambda$  of proper value, the coherence between reconstructed EEG and sEMG corresponding to the sparse expansion matrices obtained by ADMM can be increased compared to the coherence between original EEG and sEMG signals. However, the increase is rather small. It is because after the procedure of sparse representation, although some background noise has been filtered, some other uncorrelated components may not be removed. The selection of components is thus essential for further extraction of coherent components.

Fig. 1 compares the coherence around Peak 2 of subject N between reconstructed EEG and sEMG signals after coefficient selection to the corresponding coherence between original EEG and sEMG signals, as well as the corresponding coherence between reconstructed EEG and sEMG before coefficient selection when  $\lambda = 0.05$ . We can observe from these

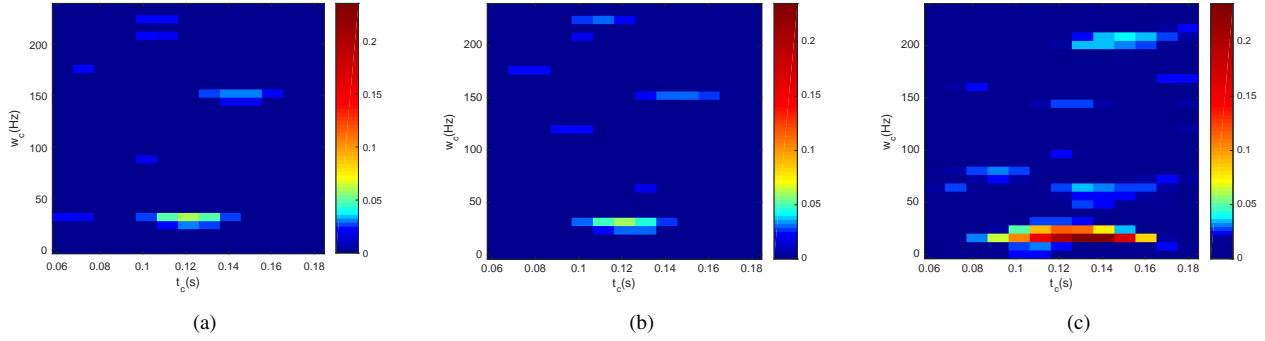


**Fig. 1:** Comparison between the CMC of original signals (left), signals obtained via the sparse representation before (middle) and after the further component selection (right). The plots correspond to 256-sample segments around Peak 2. CMC values below the 95% confidence limit are set to zero. The  $x$  axis represents the relative time within the considered segment.

**Table 1.** CMC values between EEG and sEMG signals reconstructed using their sparse expansion matrices obtained by ADMM under different values of  $\lambda$  compared to original CMC values corresponding to Peak 2 of CMC.

Subject	Coherence value					
	Original	After ADMM under different values of $\lambda$				
		0.01	0.05	0.1	0.2	0.3
B	0.1356	0.1400	0.1429	0.1359	0.1126	0.0351
J	0.0842	0.0846	0.0840	0.0829	0.0781	0.0723
K	0.1490	0.1515	0.1481	0.1330	0.1030	0.0830
L	0.0771	0.0775	0.0772	0.0767	0.0746	0.0717
N	0.0578	0.0629	0.0634	0.0661	0.0539	0.0370

figures that owing to the further component selection the overall method achieves remarkable increase of the levels of coherence. Moreover, around the coherence peak, more  $\beta$ -range coherence is brought above the significant level by this approach. Coherence increase can be observed also in frequency regions where it is typically not expected, either before or after applying the coefficient selection method, e.g. around 120 Hz in Fig. 1(b) and around 200 Hz in Fig. 1(c). Nonetheless, its level is substantially below the level of peak coherence in  $\beta$  range. A possible explanation is that although we observed CMC primarily within  $\beta$  range in this study, it does not mean there were no coherent components corresponding to other frequency ranges. The components we selected to maximize the CMC at peak frequency could also contribute to the CMC in other frequency ranges.

Table 2 shows the results of increase of CMC corresponding to Peak 2 using this method, along with the results obtained using Wavelet Threshold Denoising (WTD) and Coherent Wavelet Enhanced Independent Component Analysis (COWICA) [7]. Note that in Table 2, the best results of those achieved with *Daubechies*, *Symlets* and *Coiflet* wavelet families and different number of scales of the wavelet trans-

form are presented for WTD. Results shown for COWICA are obtained with Daubechies wavelet *db1* and 7 scales of the wavelet transform. It can be noticed that the proposed method achieves a much more pronounced increase in CMC levels than the other two methods.

**Table 2.** Increase of CMC achieved by WTD, COWICA and the proposed method based on sparse signal processing after the further component selection

Subject	Coherence increase of Peak 2 (%)		
	by WTD	by COWICA	by proposed method
B	3.69	18.81	313.57
J	5.30	21.02	64.96
K	8.99	36.71	71.48
L	5.51	15.55	118.42
N	3.27	73.48	244.98

#### 4. CONCLUSION

In this study we propose a novel method for increasing the level of coherence between EEG and sEMG signals recorded synchronously during motor control task. The method combines dictionary learning and sparse expansion techniques with a component selection algorithm to extract relevant EEG and sEMG components. Evaluations which use physiological data show that the method has the ability to achieve a substantial increase in CMC levels.

#### ACKNOWLEDGMENT

We are grateful to Professor Kerry R. Mills for his guidance.

## 5. REFERENCES

- [1] S. Baker, E. Olivier, and R. Lemon, "Coherent oscillations in monkey motor cortex and hand muscle emg show task-dependent modulation," *The Journal of physiology*, vol. 501, no. 1, pp. 225–241, 1997.
- [2] B. A. Conway *et al.*, "Synchronization between motor cortex and spinal motoneuronal pool during the performance of a maintained motor task in man," *J. Physiol.*, vol. 489, no. Pt 3, pp. 917–924, 1995.
- [3] D. M. Halliday *et al.*, "Using electroencephalography to study functional coupling between cortical activity and electromyograms during voluntary contractions in humans," *Neurosci. Lett.*, vol. 241, no. 1, pp. 5–8, 1998.
- [4] Y. Xu, V. M. McClelland, Z. Cvetkovic, and K. R. Mills, "Delay estimation between eeg and emg via coherence with time lag," in *IEEE International Conference on Acoustics, Speech and Signal Processing (ICASSP)*, March 2016, pp. 734–738.
- [5] Y. Xu, V. M. McClelland, Z. Cvetkovi, and K. R. Mills, "Corticomuscular coherence with time lag with application to delay estimation," *IEEE Transactions on Biomedical Engineering*, vol. 64, no. 3, pp. 588–600, March 2017.
- [6] V. M. McClelland, Z. Cvetkovic, and K. R. Mills, "Rectification of the emg is an unnecessary and inappropriate step in the calculation of corticomuscular coherence," *J. Neurosci. Meth.*, vol. 205, no. 1, pp. 190–201, 2012.
- [7] Y. Xu, V. M. McClelland, Z. Cvetkovi, and K. R. Mills, "Cortico-muscular coherence enhancement via coherent wavelet enhanced independent component analysis," in *39th Annual International Conference of the IEEE Engineering in Medicine and Biology Society (EMBC)*, July 2017, pp. 2786–2789.
- [8] R. N. Vigário, "Extraction of ocular artefacts from eeg using independent component analysis," *Electroencephalography and clinical neurophysiology*, vol. 103, no. 3, pp. 395–404, 1997.
- [9] T.-P. Jung, S. Makeig, C. Humphries, T.-W. Lee, M. J. Mckeown, V. Iragui, and T. J. Sejnowski, "Removing electroencephalographic artifacts by blind source separation," *Psychophysiology*, vol. 37, no. 2, pp. 163–178, 2000.
- [10] R. Vigário, J. Sarela, V. Jousmiki, M. Hamalainen, and E. Oja, "Independent component approach to the analysis of eeg and meg recordings," *IEEE transactions on biomedical engineering*, vol. 47, no. 5, pp. 589–593, 2000.
- [11] H. Nakamura, M. Yoshida, M. Kotani, K. Akazawa, and T. Moritani, "The application of independent component analysis to the multi-channel surface electromyographic signals for separation of motor unit action potential trains: part imeasuring techniques," *Journal of Electromyography and Kinesiology*, vol. 14, no. 4, pp. 423–432, 2004.
- [12] T. Xu, W. Wang, and W. Dai, "Sparse coding with adaptive dictionary learning for underdetermined blind speech separation," *Speech Communication*, vol. 55, no. 3, pp. 432–450, 2013.
- [13] M. Aharon, M. Elad, and A. Bruckstein, "K-svd: An algorithm for designing overcomplete dictionaries for sparse representation," *IEEE Transactions on signal processing*, vol. 54, no. 11, pp. 4311–4322, 2006.
- [14] D. L. Donoho, "For most large underdetermined systems of linear equations the minimal  $\ell_1$ -norm solution is also the sparsest solution," *Communications on pure and applied mathematics*, vol. 59, no. 6, pp. 797–829, 2006.
- [15] S. Boyd, N. Parikh, E. Chu, B. Peleato, and J. Eckstein, "Distributed optimization and statistical learning via the alternating direction method of multipliers," *Foundations and Trends® in Machine Learning*, vol. 3, no. 1, pp. 1–122, 2011.
- [16] G. C. Carter *et al.*, "Estimation of the magnitude-squared coherence function via overlapped fast fourier transform processing," *IEEE Trans. Audio Electroacoust.*, vol. 21, no. 4, pp. 337–344, 1973.
- [17] Z. Cvetkovic, "On discrete short-time fourier analysis," *IEEE Trans. Signal Process.*, vol. 48, no. 9, pp. 2628–2640, September 2000.
- [18] V. M. McClelland *et al.*, "Modulation of corticomuscular coherence by peripheral stimuli," *Exp. Brain Res.*, vol. 219, no. 2, pp. 275–292, 2012.